LA-UR-79-3223

MASTER

CONF-791117--12

TITLE: EXPERIMENTAL COMPARISON OF THE ACTIVE WELL COINCIDENCE COUNTER WITH THE RANDOM DRIVER

AUTHOR(S): Howard O. Menlove, Norbert Ensslin, Thomas E. Sampson

SUBMITTED TO: To be presented at the American Society Topical Conference, Measurement Technology for Safeguards and Materials Control, at Kiawah Island, SC, November 26-29, 1979.

University of California

LOS ALAMOS SCIENTIFIC LABORATORY
Post Office Box 1663 Los Alamos, New Mexico 87545
An Affirmative Action/Equal Opportunity Employer

UNITED STATES
DEPARTMENT OF ENERGY

MASTER

EXPERIMENTAL COMPARISON OF THE ACTIVE WELL COINCIDENCE COUNTER WITH THE RANDOM DRIVER

by

Howard O. Menlove, Norbert Ensslin, and Thomas E. Sampson
Los Alamos, New Mexico 87545

ABSTRACT

A direct comparison has been made between the IAEA Active Well Coincidence Counter (AWCC) and the LASL Random Driver at CMB-8. The comparison included an experimental evaluation of precision, counting rate, accuracy, penetrability, stability, and the effect of sample inhomogeneity.

Samples used in the evaluation included highly enriched U_3O_8, U_3O_8 mixed with graphite, highly enriched uranium metal discs, and depleted uranium metal. These materials are typical of the samples of interest to the IAEA inspectors.

We concluded from these investigations that the two instruments had very similar performance characteristics with the Random Driver giving better penetrability and the AWCC giving better stability.

KEYWORDS: Nondestructive assay, uranium, random driver, neutron, coincidence counter, stability, precision, calibration

INTRODUCTION

In recent years, random driver (RD) type instruments have been widely used for the nondestructive assay (NDA) of ^{235}U. There have been several versions of random drivers;[1] some designed and built by LASL and some by commercial instrumentation vendors. The paper by Paul Goris in Session IV of this symposium described the application of a commercial random driver to the NDA of ^{233}U. The different RD units have generally improved over the years with better detectors, electronics, and data analysis techniques. However, this type of system is not readily adaptable to portable applications for field inspections because of its weight and complexity.

The Active Well Coincidence Counter[2] uses a combination of a small AmLi neutron interrogation source and a ^3He thermal-neutron well coincidence counter. This Active counter can be used for uranium samples, including high gamma-ray background materials such as ^{233}U-Th fuels. The present AWCC was developed to be more lightweight and portable than the conventional fast random driver assay system.

The purpose of the present paper is to make a direct experimental comparison of the RD and the AWCC. The performance parameters of interest in the comparison are:

1. counting rates,
2. precision,
3. stability,
4. response linearity, penetrability,
5. geometric effects,
6. sample inhomogeneities and matrix effects.

Samples that were available for the comparison included highly enriched U_3O_8 in recovery cans, U_3O_8 mixed with graphite, and uranium metal discs (93.15% ^{235}U) similar in size to the "buttons" and ingots used for fuel fabrication. The mass of the samples ranged from 250 to 4000 g U.

RANDOM DRIVER DESCRIPTION

The Random Driver is typically used to determine the enriched uranium content of oxide, metal, or residue samples.[3] Typical container sizes are 5 to 10 liters capacity. AmLi random neutron sources are used to induce fisson reactions in the ^{235}U present in the material. Relatively few fissions occur in the ^{238}U because the neutron energy spectrum of the AmLi sources (0.3 MeV average) is below the fission threshold for ^{238}U. Also, the spontaneous fission rate of ^{238}U is very low. The fissions induced in ^{235}U are observed by coincidence counting the time-correlated fission neutrons with two 5 x 25 x 50 cm Pilot F fast plastic scintillators, located on opposite sides of the assay chamber as shown in Fig. 1. By requiring the detection of neutrons in both scintillators within 45 nanoseconds, it is possible to distinguish fission events from randomly produced AmLi source neutrons. The coincidence counting rate is proportional to the quantity of ^{235}U in the material being assayed, and thus provides a measure of the uranium content.

A number of features are incorporated in the design of the RD to reduce potential sources of assay bias. The interrogating neutrons are not thermalized, and the assay chamber is lined with boral to absorb low-energy neutrons, thus ensuring good neutron penetrability through the sample. The detectors are also shielded with 5 cm of lead, because the fast plastic scintillators are sensitive to energetic gamma rays as well as neutrons. This lead eliminates the gamma rays from the AmLi source and some of the induced fission gamma-rays from ^{235}U. The attenuation of gammas in most large samples is greater than the attenuation of neutrons. To make assays less dependent on sample density and composition, the RD discriminates against gamma rays by the use of lead and by time-of-flight. Gamma ray signals are detected in the scintillators in the first 2-3 ns, whereas neutron flight times are typically 20-40 ns. A time window of 5-45 ns is used to accept most (n,n) coincidences and reject most (γ,γ) coincidences. For typical energy thresholds of 650 keV for neutrons and 220 keV for gammas, the RD response consists of 78% (n,n) coincidences and 22% (n,γ) coincidences.[4]

Two techniques are used to reduce the effects of loading differences between samples. The sample is rotated during assay to minimize the effect of asymmetric loading of material within the container, and the AmLi sources are positioned to produce a nearly uniform vertical response profile over the typical range of container fill heights (2-20 cm). There is a 3-5% variation in RD response as a function of height, as determined by moving a small sample along the central axis of the sample chamber. For large samples the total integrated response is constant to 1% or less over the range of fill heights.

The effect of introducing moderating material into the assay chamber is to reduce the energy of the interrogating spectrum, which increases the rate of induced fission in ^{235}U. Light element moderating material can appear either as matrix or in polyethylene containers and bags. Because the type of container (i.e., metal or polyethylene) used for most material being assayed is dictated by the process stage in which the material occurs, assay data should normally be corrected for perturbations caused by moderating material in the sample chamber. This correction is based on the response of two ^3He proportional counters, located adjacent to the sample assay position, which monitor the interrogating neutron flux.

Elimination of some sources of assay bias by the instrument design features and corrections described above has reduced the number of physical standards required for calibration of the RD. However, experience with a wide variety of sample types has shown that widely different materials require different calibration curves to obtain good accuracy. The RD described in this report has separate calibration curves for pure uranium oxide, oxide mixed with graphite, uranium in hydrofluoric slag, and reduction metal residues.

ACTIVE WELL COINCIDENCE COUNTER

The basic principle of the AWCC is the same as the RD. That is, fast-neutron interrogation using a random neutron source (e.g., AmLi) and counting the induced fission reactions using coincidence techniques to suppress the signal from the random interrogation source. The primary difference is that the AWCC uses ^3He detectors which are sensitive to neutrons after they have slowed. This necessitates the use of relatively long (32-64 µs) coincidence time gates resulting in a large fraction of accidental coincidence events for high counting rates. To help alleviate this problem, we have positioned the AmLi source inside CH_2 shielding (the end plugs) as shown in Fig. 2 to reduce the accidental pileup rate. With this technique, the induced signal-to-interrogation neutron background ratio is improved by a factor of ten.

The AWCC has been designed to take advantage of the portable electronics package[5] that was developed for the HLNCC. To keep this initial model as simple as possible and to take direct advantage of the previously developed electronics package, no neutron flux monitor has been incorporated into the present AWCC. Flux monitors are often used with active neutron assay units to make corrections for neutron self-shielding or for neutron moderation in hydrogeneous matrix materials. Operational experience with the present model will be used to evaluate the need for a flux monitor in more advanced models.

Normally the sample cavity wall of the AWCC is lined with a 2.54-cm-thick nickel reflector to give a more penetrating neutron interrogation. However, the sample cans for the U_3O_8 plus graphite were so large (20-cm diam) that it was necessary to remove the nickel liner and the top and bottom CH_2 discs (7.6-cm-thick) to accomodate the cans. The removal of the nickel results in some loss of penetrability. The counter was returned to the configuration shown in Fig. 2 for the measurements on the HEU metal discs. There is a sleeve of Cd in the detector sample well to remove thermal neutrons from the interrogation flux and to improve the shielding between the ^3He detectors and the AmLi source.

To obtain a more uniform spatial interrogation, two neutron sources of similar yield are used. One is in the lid and one is in the bottom plug as shown in Fig. 2. The use of two sources results in a rather uniform vertical response.

The unit uses 42-^3He gas (4 atm pressure) tubes that are 2.54 cm diameter and 50.8 cm long (active length). This detector configuration gives an absolute efficiency of approximately 30% for counting fission spectrum neutrons.

The electronics unit is directly interfaced to the HP-97 programmable calculator shown in Fig. 3. A microprocessor in the unit reads out the run time, total counts, reals plus accidental counts, and accidental counts to the HP-97. The HP-97 is then used to reduce the data using the software package selected by the operator.

Table I gives the specifications for both the RD and the AWCC showing the major physical differences in the two systems. The weight and size of the AWCC is considerably less than for the RD.

EXPERIMENTAL PROCEDURES

For the comparison, the AWCC was taken to the uranium recovery plant at LASL, where the CMB-8 Random Driver shown in Fig. 4 is in routine use. Thus, both systems were operating side-by-side to obtain the same environmental factors. The samples were alternatively counted in the RD and the AWCC for the same time intervals - typically 1000 s. Repeat runs were performed on the lower mass samples to improve the counting statistics.

The samples selected for the measurement were those normally used for the calibration of the RD (U_3O_8) plus the HEU metal discs that were prepared for IAEA detector calibration. Also, depleted uranium metal discs of the same size as the HEU discs were mixed with HEU discs to create inhomogeneities in the sample.

To check the stability of the systems, cyclic runs were performed over two nights and over a three day weekend. High mass samples were used for these runs to give good counting statistics to better check the precision.

The primary evaluation considered the RD coincidence response directly without making corrections for the flux monitor or temperature sensor. This was to permit a direct comparison with the AWCC coincidence response which has no correction sensors in the present model. The data shown in the graphs and tables corresponds to the uncorrected response from both systems. The magnitude of the correction factors for the RD were observed to be small and rather uniform over each of the sample categories.

TABLE I

RD AND AWCC SYSTEM SPECIFICATIONS

	RD	AWCC
Number of AmLi sources	2	2
Total source strength	10^6 n/s	10^5 n/s
Interrogation energy	Fast neutron	Fast neutron
Detector type	Plastic scintillators	^{3}He tubes
Counting	Fast neutrons and gamma rays	Thermalized neutrons
Response signal	Fast coincidence	Slow coincidence (auto-correlation)
Coincidence gate	∿ 45 ns	∿ 64 μs
Body weight	1150 kg	125 kg
Electronics	2 NIM BINS plus minicomputer	HLNCC package plus HP-97

RESULTS

U_3O_8-Large Containers

The RD located at the LASL uranium recovery facility is normally used to measure the ^{235}U content of U_3O_8 in stainless steel cans that are ∿ 20-cm-diam x 25 cm tall. This material is in two sample categories - each having its own set of standards. The first is pure U_3O_8 ranging in mass from 250 to 4000 g uranium (∿93% enriched in ^{235}U). The standards of this type material that were used for the comparison are listed in Table II. The uranium is very concentrated and fills only the bottom few centimeters of the can resulting in a "pancake" shaped sample. The U_3O_8 had a density of approximately 2.38 g/cm^3 resulting in a ^{235}U density of 1.96 g/cm^3. This density was basically the same for all of the U_3O_8 standards with only the fill height changing as the sample mass increased.

The set of U_3O_8 standards mixed with graphite are listed in the bottom section of Table II. In this case the graphite fills most of the volume resulting in a low ^{235}U density. The mass of the uranium ranged from 234 to 4000 g. The ^{235}U densities were 3 to 30 times lower than for the pure U_3O_8 material. Also, the densities and fill heights had large variations as given in Table II. The large quantities of graphite in these containers had a significant effect on the observed signal for both assay systems.

Random Driver Results

The net coincidence response of the RD as a function of uranium content is shown in Fig. 5. All of the data points lie on a smooth curve which has the functional form aU/1+bU for uranium values less than 2000 g. For the 4000 g sample, the multiplication gives a slight increase in the coincidence response.

The curve for the U_3O_8 plus graphite falls below the curve for pure U_3O_8 for the RD. This result is somewhat surprising because the graphite will increase the interrogation flux density and increase the number of slow neutrons which have a high fission cross section for ^{235}U. However for the RD, the graphite has the opposite effect on the

TABLE II

STANDARD SAMPLE CHARACTERISTICS

Sample ID	Net Wt. (g)	Fill Ht. (cm)	Diam (cm)	gU	Enrichment (%)	$\rho^{235}U$ (g/cm^3)
Pure U_3O_8						
TRN-250	296	0.46	18.2	250	93.14	1.94
TRN-500	591	0.91	18.2	500	93.14	1.96
TRN-1000	1183	1.82	18.2	1000	93.14	1.96
TRN-1500	1774	2.73	18.2	1500	93.14	1.96
TRN-2000	2366	3.64	18.2	2000	93.14	1.96
U_3O_8 Plus Graphite						
STD-234	4678	13.5	20.0	234	92.83	.0512
STD-468	4678	12.0	20.0	468	92.83	.115
STD-500	7005	19.3	20.0	500	92.88	.0765
STD-846	4230	10.0	20.0	846	92.83	.250
STD-100	7335	1[illegible].6	20.0	1000	92.88	.159
STD-1591	4679	12.5	20.0	1591	92.83	.376
STD-2000	7640	19.0	20.0	2000	92.88	.311
STD-4000	9691	18.0	20.3	4000	92.88	.657

counting channel. That is, the induced fission neutrons and gamma rays have a more difficult time being counted by the plastic scintillators. The cans contain 4-6 kg of graphite which both absorbs fission gamma rays in transit to the scintillators and slows down the fast neutrons so that they are below the counting energy-threshold. This graphite has the opposite effect on the response for the AWCC which will be discussed in the next section.

The net coincidence response for the U_3O_8 samples are listed in Table III. The error corresponds to the calculated standard deviation for a 1000 s run. For the low mass samples, several measurements were performed to obtain better precision than the value listed in the table.

The last column in Table III gives the coincidence rate per gram sample. This is an indication of the penetrability of the interrogation flux. A linear calibration curve would correspond to a constant value for the response per gram. The pure U_3O_8 curve is more linear than the graphite curve because the graphite moderates the interrogation neutrons resulting in more low-energy neutrons and thus more self-shielding in the ^{235}U.

Active Well Coincidence Counter Results

The results for the same set of standards measured with the AWCC are shown in Fig. 6. These curves are more nonlinear than the corresponding curves for the RD. This indicates a softer interrogation neutron spectrum for the AWCC. The reason for this is the large amount of hydrogen in the CH_2 end plugs and detector walls.

The curve for the U_3O_8 plus graphite is above the U_3O_8 curve. We expect this to be the case because the large quantity of graphite increases the low energy neutron flux. As opposed to the RD, the graphite has little or no effect on the efficiency of the AWCC for counting the induced fission neutrons.

The data point at 1591 g U falls significantly below the curve through the other data points. A likely reason for the low response is that this can contains less graphite than the other cans with similar amounts of uranium resulting in less neutron moderation. Also, the graphite acts as a diluting agent for the U_3O_8 and less graphite means a higher concentration of U_3O_8 and thus more self-shielding. The AWCC is more sensitive to this type problem than the RD. The large sample cans made it necessary to remove the nickel liner from the AWCC and this increased the self-shielding problems.

TABLE III

RANDOM DRIVER MEASUREMENT RESULTS FOR U_3O_8 AND U_3O_8 PLUS GRAPHITE STANDARDS

Sample I.D.-g U	Coincidence Rate (s^{-1})	Standard Deviation (1000 s)	$\frac{\text{Counts}}{\text{s·gU}}$ x 1000
U_3O_8			
TRN-250	4.90	5.2%	19.6
TRN-500	9.75	2.0%	19.5
TRN-1000	18.7	1.5%	18.8
TRN-1500	27.3	1.1%	18.2
TRN-2000	35.3	0.88%	17.6
U_3O_8 plus Graphite			
STD-234	4.27	5.8%	18.3
STD-468	8.56	3.0%	18.3
STD-500	8.84	2.9%	17.7
STD-846	14.7	1.8%	17.4
STD-1000	16.8	1.6%	16.8
STD-1591	26.3	1.1%	16.5
STD-2000	31.5	0.98%	15.8
STD-4000	57.8	0.62%	14.5

The results of the AWCC measurements are listed in Table IV, and we see that the net coincidence rate for the AWCC is approximately 6 times higher than for the RD even though the AmLi source strength is a factor of ten smaller. The reason for this is the higher detector efficiency and the softer interrogation flux. It should be noted that the standard deviations for both the AWCC and RD are about the same in spite of this higher count rate. This is because of the high accidental coincidence rate in the AWCC contributing to the statistical error. The coincidence time gate in the AWCC is 64 μs compared with about 45 ns for the RD.

HEU Metal Discs

The high enrichment metal discs used in the present experiment are similar to metal buttons of interest in inventory inspections. The two diameters (6- and 7-cm) for the discs were used to check the effect of diameter variations in the measurements.

To obtain the mass range from approximately 500-4000 g U, the discs were stacked on top of each other to form a cylinder with heights varying from 1-cm to 7-cm. The uranium metal had a density of 18.7 g/cm^3 resulting in a ^{235}U density of 17.5 g/cm^3. To avoid oxidation and contamination by the uranium, the discs were coated with a thin nickel plate.

Random Driver Results

The samples were counted in the RD with no change in the detector configuration used for the large U_3O_8 cans. The results of the measurements are given in Table V. The response per g U of a single disc (17.2) is somewhat less than the response per g U for the U_3O_8 samples (19.5 for TRN-500). This reduction is likely caused by neutron or gamma self-shielding in the higher density metal.

As the sample mass increases from 1 disc to 7 discs, the response per gram increases from 17.2 to 20.7 or a 20% increase. This is caused by the multiplication of the induced fission neutrons.

Figure 7 gives a plot of the net coincidence rate as a function of uranium mass. The curve is fit through the data for the 6-cm-diam discs. The larger 7-cm discs had an average response per gram that was only 1.6% higher than the smaller diameter discs.

TABLE IV

AWCC MEASUREMENT RESULTS FOR U_3O_8 AND U_3O_8 PLUS GRAPHITE STANDARDS

Sample I.D.-g U	Coincidence Rate (s^{-1})	Standard Deviation (1000 s)	$\frac{\text{Counts}}{\text{s·gU}}$ x 1000
U_3O_8			
TRN-250	24.2	6.4%	96.8
TRN-500	42.9	3.8%	85.9
TRN-1000	88.0	1.9%	88.0
TRN-1500	124.9	1.4%	83.3
TRN-2000	153.3	1.2%	76.6
U_3O_8 Plus Graphite			
STD-234	33.4	5.1%	142.6
STD-468	56.0	3.1%	119.7
STD-500	61.9	2.8%	123.8
STD-846	96.6	1.9%	114.2
STD-1000	109.6	1.6%	109.6
STD-1591	147.3	1.2%	92.6
STD-2000	185.5	1.0%	92.7
STD-4000	300.2	0.61%	75.0

TABLE V

HEU METAL BUTTONS MEASURED WITH THE RANDOM DRIVER

Sample Size diam x ht. (cm)	Sample Mass[a] (g U)	Coincidence Rate (s^{-1})	Standard Deviation (1000 s run)	$\frac{\text{Counts}}{\text{s·g U}}$ x 1000
6 x 1	528	9.10	4.2%	17.2
6 x 2	1055	18.16	1.6%	17.2
6 x 3	1583	28.44	1.1%	18.0
6 x 4	2112	39.04	0.80%	18.5
6 x 5	2640	51.30	0.65%	19.4
6 x 6	3168	63.81	0.54%	20.1
6 x 7	3692	76.43	0.46%	20.7
7 x 1	718	12.36	2.16%	17.2
7 x 2	1434	25.36	1.15%	17.7
7 x 3	2152	40.94	0.78%	19.0
7 x 4	2870	57.69	0.60%	20.1

a) Uranium metal samples 93.14% enriched in ^{235}U.

b) Corresponds to relative error in net coincidence rate considering only counting statistics.

The upward curvature of the response from multiplication is evident. Techniques are under development to make automatic corrections in the data for multiplication.

Active Well Coincidence Counter Results

For the HEU disc measurements, the AWCC was returned to its normal configuration as shown in Fig. 2. This smaller sample cavity increases the irradiation efficiency and the nickel liner improves the penetrability of the neutron flux.

Table VI gives the results for the different sample masses. The coincidence response per gram for a disc (87.2) is very close to the response for the U_3O_8 samples (85.9 for TRN-500); however, this is only a "coincidence" because the detector and end plug configuration was different for the two cases.

The response per gram changes by only 8% in going from 1 disc to 7 discs. There is a cancellation of self-shielding and multiplication effects. For the lower mass region (<1500 g U) the self-shielding dominates resulting in a decline of the response per g U, but for the higher mass values (>2000 g U) the multiplication dominates resulting in an increase in the response per g U. The average difference in response per g U from the mean was only 2.7%.

A plot of the coincidence rate versus the response is shown in Fig. 8. The curve is fit through the data points for the 6-cm- diam discs. The 7-cm discs fall slightly above the curve. The average rate per gram for the 7-cm discs is 2.2% higher than for the 6-cm discs.

Inhomogeneities

A pair of 6-cm-diam x 1-cm-thick depleted uranium metal discs were used to check the sensitivity of the assay systems to inhomogenous samples. Two HEU metal discs were measured in the following configurations: a) two HEU discs with no depleted uranium (DU) discs, b) two HEU discs inside the DU discs, and c) two HEU discs outside the DU discs.

We observed that the DU disc inhomogeneities change the results by only approximately 2% for the AWCC, but the change is approximately 5% for the RD. The RD has the larger perturbation because gamma rays contribute to its signal and the DU absorbs some of the gamma rays before they reach the scintillators.

TABLE VI

HEU METAL BUTTONS MEASURED IN AWCC WITH Ni LINER IN WELL

Sample Size diam x ht. (cm)	Sample Mass[a] (g U)	Coincidence Rate (s^{-1})	Standard[b] Deviation (1000 s run)	$\frac{\text{Counts}}{\text{s·g U}}$ x 1000
6 x 1	524	45.72	3.2%	87.2
6 x 2	1055	86.289	1.55	81.8
6 x 3	1583	127.55	1.2%	80.6
6 x 4	2111	170.30	0.85%	80.7
6 x 5	2636	218.73	0.74%	83.0
6 x 6	3164	268.33	0.64%	84.8
6 x 7	3692	318.33	0.55%	86.2
7 x 1	718	66.22	2.3%	92.2
7 x 2	1434	116.19	1.4%	81.0
7 x 3	2152	179.11	0.92%	83.2
7 x 4	2870	246.65	0.69%	85.9

a) Uranium metal samples 93.17% enriched in ^{235}U.

b) Corresponds to relative error in net coincidence rate considering only counting statistics.

Additional tests were performed where the U_3O_8 contents of sample TRN-2000 were forced to one side of the can. The measured rate was compared with the normal sample geometry. In this case the RD had less of a perturbation than the AWCC. This is partly because the RD has a more penetrating interrogation flux than the AWCC and partly because there is less radial geometric variation in the RD. The sample rotates past the interrogation sources which averages out radial variations in the RD; whereas, there is no sample rotation in the AWCC, and the interrogation flux decreases with radial distance from the central axis of the well.

Measurement Precision and Stability

A series of measurements were performed overnight and over the weekend to check the precision and stability of the two systems. Normally the 1500 g U or 2000 g U samples were used in the counters to give the coincidence response.

The results of the measurements are given in Table VII. The observed standard deviations are very close to the standard deviations predicted by counting statistics for the AWCC. The standard deviation in parentheses for the RD corresponds to the measured value after making corrections with the temperature sensor and the minicomputer. For cases with better statistical precision (e.g., the 10,000 s runs), the observed RD deviations are larger than would be expected from counting statistics alone. The cause of the instability is likely to be the scintillator-photo tube system. The stability of the ^{3}He detector system in the AWCC is very good.

CONCLUSIONS

There are many characteristics and parameters to be considered in the comparison of the RD and AWCC systems. The relative importance of these parameters depends on the application and constraints on the user. A brief summary follows for the major parameters of interest.

Counting Rates

The net coincidence counting rate is approximately 18 x 10^{-3} counts/s·gU for the RD and approximately 84 x 10^{-3} counts/s·gU for the AWCC. However, this difference in rate is not important because the statistical error is dominated by the accidental coincidence rate which is considerably h[illegible] for the AWCC.

TABLE VII

STABILITY RESULTS FOR AWCC AND RD

	Net Coincidence Counts	
	AWCC	RD [a]
Wednesday Overnight		
(4000 s runs - 15 h period)		
1σ predicted	0.55%	0.42%
1σ observed	0.59%	0.82%(0.54%)
Thursday Overnight		
(4000 s runs - 15 h period)		
1σ predicted	0.58%	0.42%
1σ observed	0.59%	0.45%(0.40%)
Friday - Monday		
(10000 s runs - 60 h period)		
1σ predicted	0.26%	0.26%
1σ observed	0.28%	1.04%(0.96%)

a) The 1σ value in parenthesis for the RD corresponds to the standard deviation of the coincidence count after making the temperature correction with the temperature sensor and minicomputer.

The fact that the AWCC uses AmLi sources that are an order of magnitude smaller than the RD is important for portable applications.

Precision

The precision is linked to the net coincidence counting rate but it also includes the background rates and the electronic stabilities. The observed precision of the RD and the AWCC were essentially the same (approximately 4-0.5%) for the counting intervals (approximately 1000 s) and mass range (500-4000 g U) of the present comparison. For higher masses or longer counting times, the statistical precision would drop below approximately 0.5% and the AWCC would have some advantage because of its better stability.

Other versions of random drivers that do not have the Pb shielding and gamma-ray time gate rejection, have a higher counting rate and better statistical precision. However, the penetrability/linearity is then worse and RD stability limits the observed precision in any case.

Penetrability and Linearity

Because of the large quantities of iron and lead close to the AmLi source and sample chamber, the RD has a harder neutron interrogation flux than the AWCC. This is demonstrated by the calibration curves for U_3O_8 where the linearity is better for the RD than the AWCC. The better penetrability of the RD makes it possible to tolerate a larger variation in certain types of sample inhomogeneities.

Geometric Effects

Changes in coincidence rates because of sample position variations or geometric effects were only briefly studied in the present work. The two source approach to flatten the spatial response is used in both instruments. The response variation as a function of fill height or vertical position is very small and essentially the same for both systems. The RD incorporates a rotating sample holder and side mounted neutron sources to reduce the effects of radial sample variations. The AWCC does not have this feature for two reasons. One is to keep the system simple from a mechanical standpoint, and the other is that the AmLi sources are mounted on the center axis of the AWCC to take advantage of the end plug shielding of the AmLi background neutrons.

Because of the above reasons and the larger sample cavity of the RD, that system is somewhat less subject to sample geometric effects.

Stability

One of the reasons for selecting ^{3}He tubes for the AWCC was their excellent stability and their insensitivity to gamma rays. For high precision counting ($1\sigma < 0.5$-1%) or applications with long periods between calibrations, the AWCC has better performance than the RD. The RD system uses plastic scintillator-phototube detectors which are subject to temperature variations and radiation fatigue. A temperature sensor is incorporated into the system and computer based corrections are made for these effects.

Matrix Effects and Flux Monitors

The effects of matrix materials in the sample and the role of the flux monitor were only lightly studied in the present comparison. This was because of the limited sample categories and the lack of a flux monitor in the AWCC.

The primary function of the ^{3}He flux monitor in the RD is to make corrections for hydrogen that might be present in the sample. Because there was no significant amount of hydrogen in the standards used in this comparison, the flux monitor correction was not large. However, if assay samples have moisture content or a large amount of plastic bagging material, a flux monitor might be required to indicate the problem and make appropriate corrections.

The harder neutron interrogation spectrum of the RD makes it less sensitive to inhomogeneities that effect the interrogation neutrons such as self-shielding in lumps of fissile material. However, the AWCC is less sensitive to matrix materials that effect the counting of the induced fission reactions. Examples of this are density variations in the matrix materials which change the gamma-ray absorption and/or the fission neutron moderation.

In summary there is not a consistent advantage of one system over the other with respect to matrix effects. If the samples contain a significant amount of moisture, a flux monitor should be used, or if the fissile density is low, thermal-neutron interrogation can be used to override the hydrogen effect.

Portability

The relative portability of the two systems was only indirectly checked in the present work. That is, the AWCC was carried to the site of the RD rather than the other way around.

In all factors which pertain to portability, the AWCC is better. The key parameter is the weight and the AWCC is roughly a factor of ten lighter. The size of the AWCC electronics is about an order of magnitude smaller than for the RD. However, the RD electronics could be reduced with sufficient effort. The AWCC is more rugged, stable, less complex, and less sensitive to temperature variations than the RD. Also, when the AWCC is turned on at a new location, the warmup time for the electronics is only a few minutes compared with several hours for the RD. The factor-of-ten smaller Am-Li source strength is another advantage of the AWCC with respect to transportation logistics.

In summary, the performance characteristics of the RD at CMB-8 and the AWCC are quite similar with respect to precision and sensitivity. The AWCC has many obvious advantages for portable applications as detailed above. For in-plant or fixed-site applications the RD has the advantage of better neutron penetrability. Also the minicomputer based data analysis system can be used for measurement control functions that are not possible with the smaller portable electronics. For samples with high gamma-ray backgrounds such as irradiated fast critical assembly plates and ^{233}U-Th fuel materials, the AWCC has the advantage of being insensitive to the gamma-ray backgrounds.

IAEA inspector applications normally require equipment that can be easily moved from one site to another, and thus the AWCC more closely meets their need.

ACKNOWLEDGEMENTS

The authors would like to thank John Foley and Merlyn Krick for their help in the design of the instrumentation and H. R. Baxman for his assistance in the preparation of the standards and use of the CMB-8 facility.

REFERENCES

1. T. L. Atwell, J. E. Foley, and L. V. East, "NDA of HTGR Fuel Using the Random Driver," Journal of the Institute of Nuclear Materials Management, VOl. III, No. III, pp. 171-188 (1974).

2. Howard O. Menlove, "Description and Operation Manual for the Active Well Coincidence Counter," Los Alamos Scientific Laboratory report LA-7823-M (1979).

3. D. Langner, T. L. Atwell, T. R. Canada, N. Ensslin, L. Cowder, T. Van Lyssel, and H. R. Baxman, "The CMB-8 Material Balance System Measurement Control Program," Los Alamos Scientific Laboratory report (1979).

4. D. M. Lee, N. Ensslin, C. Shonrock, and T. Van Lyssel, "Random Driver Studies," Los Alamos Scientific Laboratory report LA-7211-PR, Sept.-Dec. 1977, p. 14.

5. Merlyn Stewart Krick and Howard O. Menlove, "The High-Level Neutron Coincidence Counter (HLNCC): Users' Manual," Los Alamos Scientific Laboratory report LA-7779-M (1978).

FIGURE CAPTIONS

Figure 1

Random Driver (RD) counting chamber - legend: A. scintillator assembly, B. source, C. base, D. base skirting, E. front maintenance panel, F. sample platen, G. lid, H. top cover, I. casters, J. weighing mechanism, K. door, L. steel shielding, M. boral shielding, N. source tailoring container.

Figure 2

Schematic diagram of Active Well Coincidence Counter (AWCC) in its normal configuration for counting small samples.

Figure 3

Photograph of AWCC system complete with detector body and cart, electronics package and HP-97 calculator for automated data readout and analysis.

Figure 4

Photograph of RD system at CMB-8 including detector body, minicomputer, electronics rack and TSI terminal.

Figure 5

Random Driver response vs g U for highly enriched U_3O_8 powder and U_3O_8 mixed with a graphite matrix.

Figure 6

AWCC response vs g U for highly enriched U_3O_8 powder and U_3O_8 mixed with graphite.

Figure 7

Random Driver response vs g U for HEU metal buttons.

Figure 8

AWCC response vs g U for HEU metal buttons.

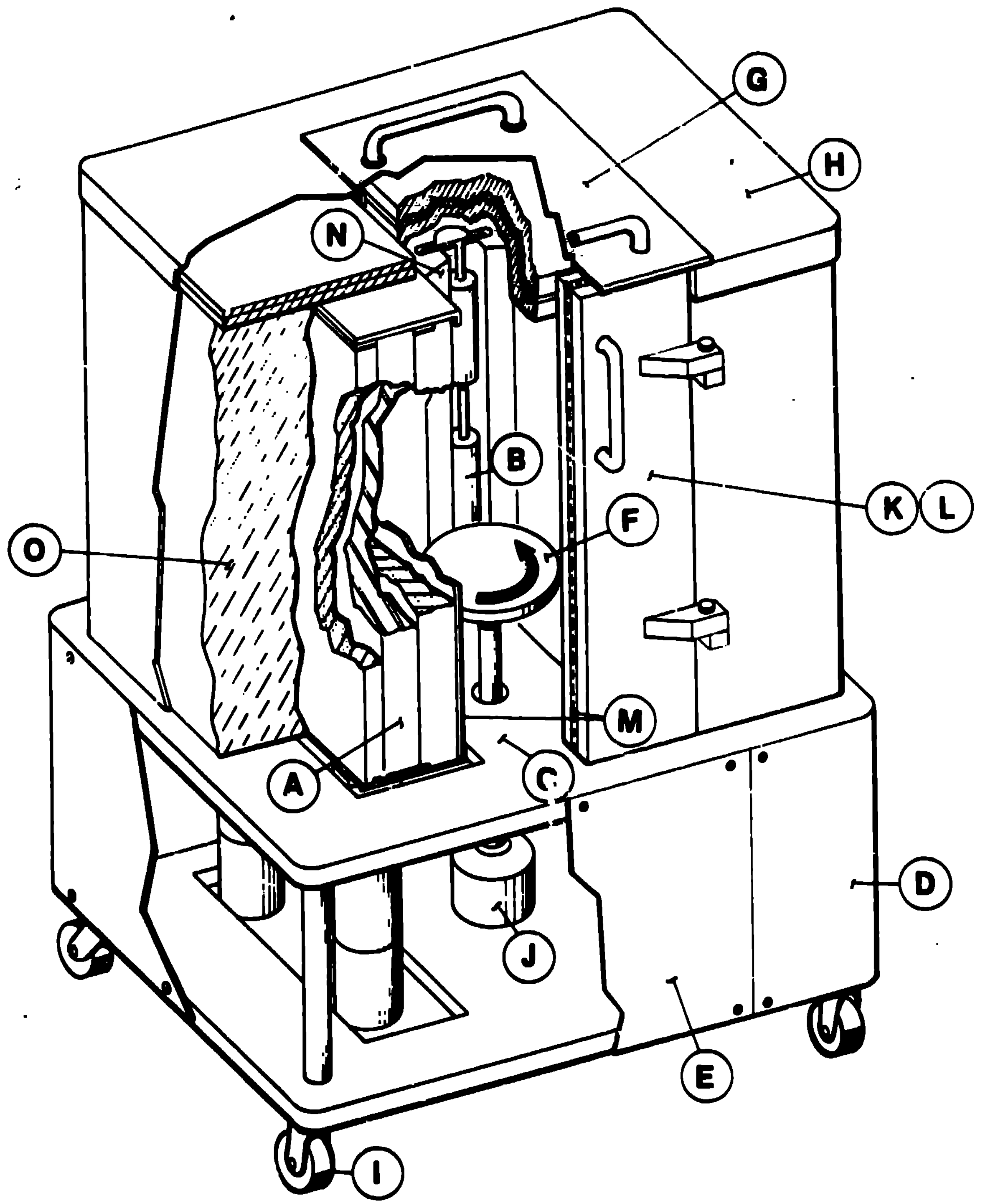
G
H
N
B
K L
O
F
M
A
C
D
J
E
I

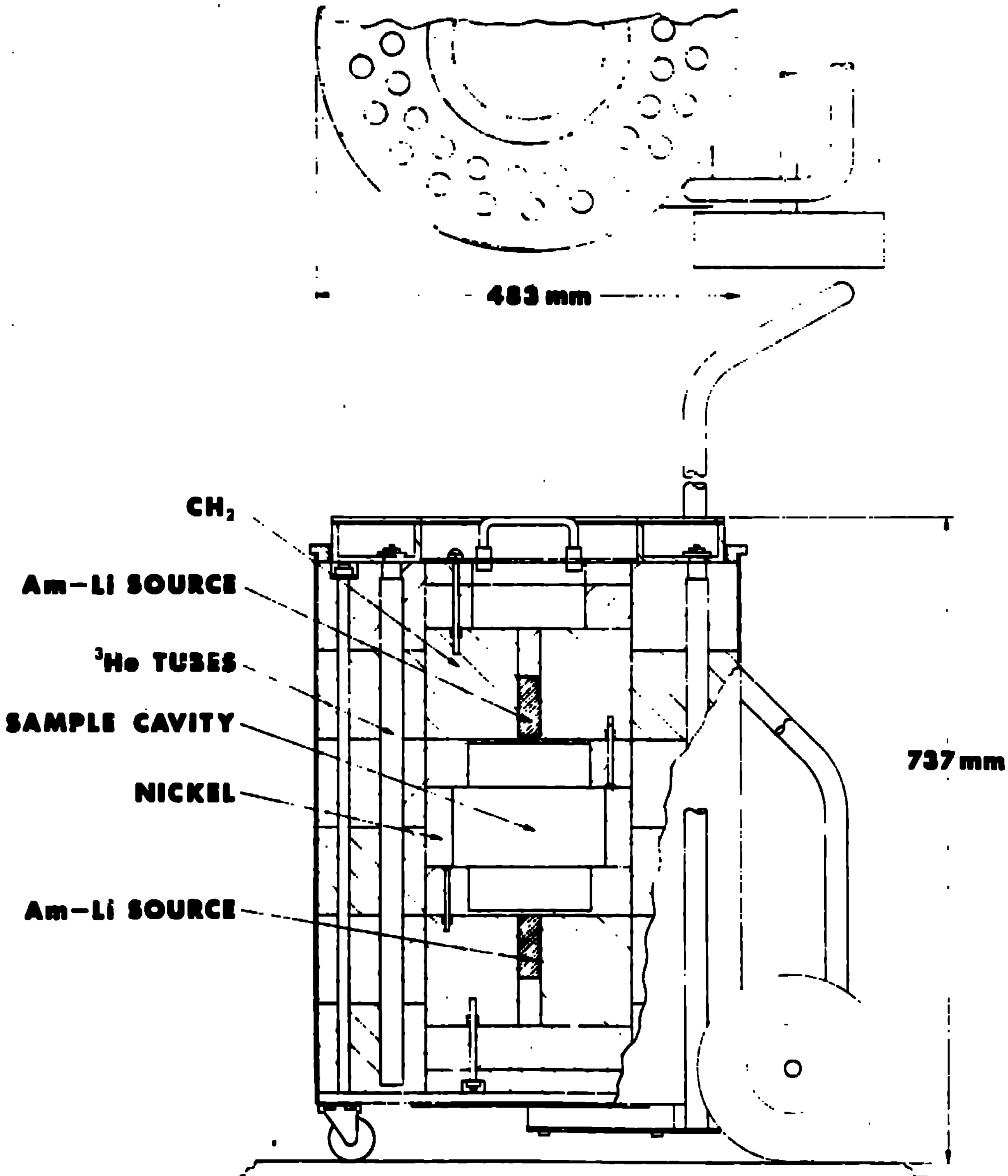

ACTIVE WELL COINCIDENCE COUNTER MOD II

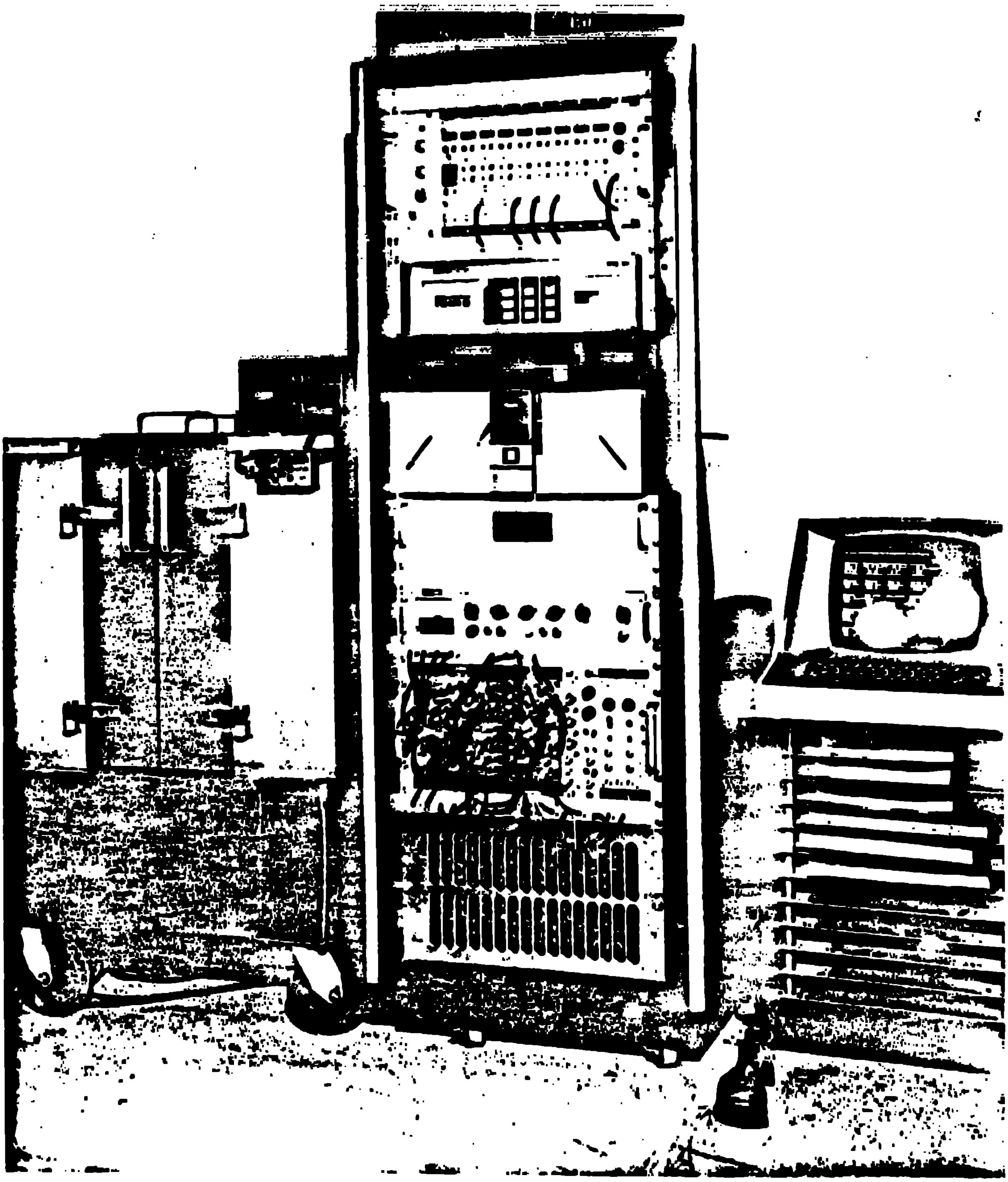

BLANK PAGE

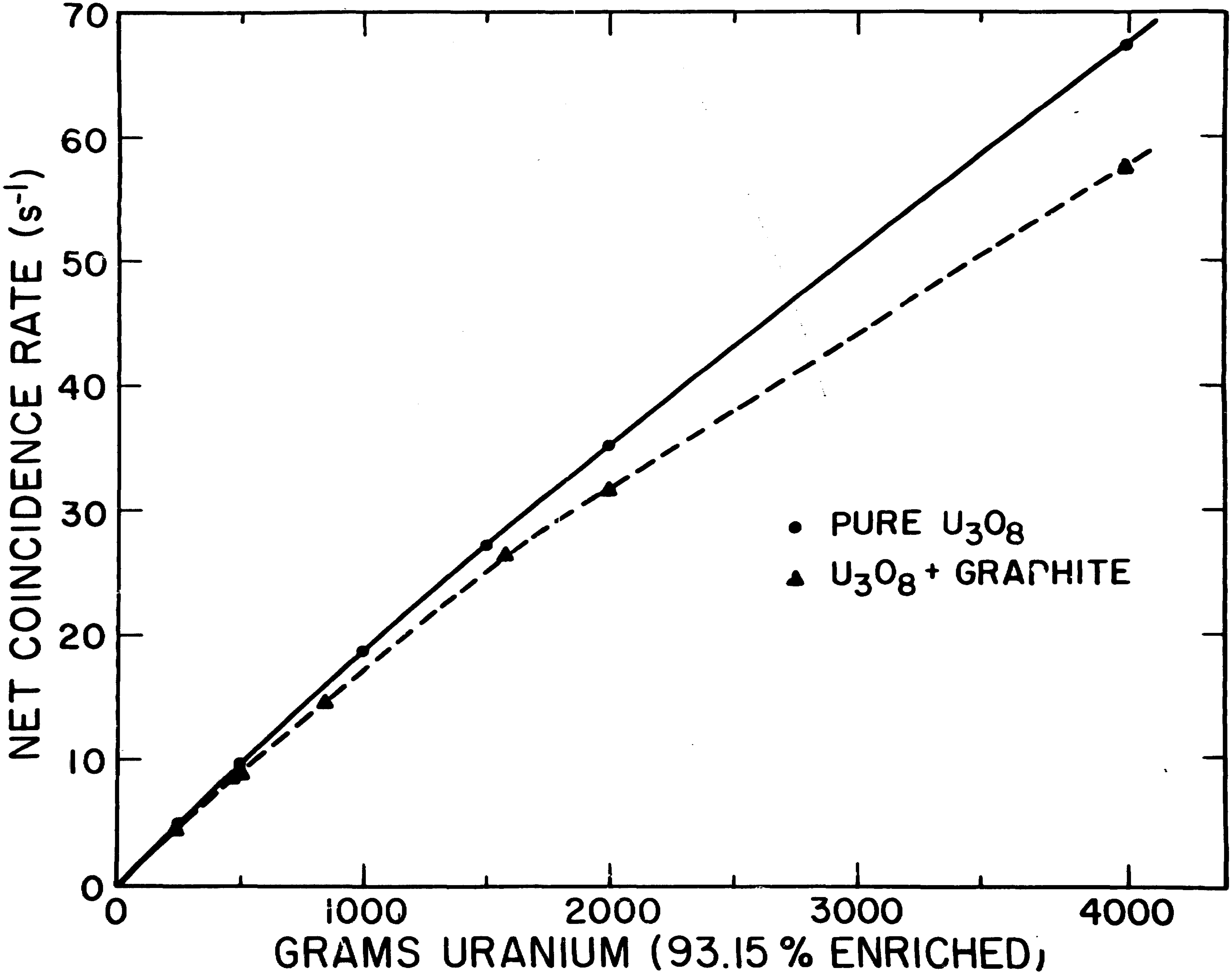

NET COINCIDENCE RATE (s^{-1})
0
10
20
30
40
50
60
70
0
1000
2000
3000
4000
GRAMS URANIUM (93.15 % ENRICHED)
PURE U_3O_8
U_3O_8 + GRAPHITE

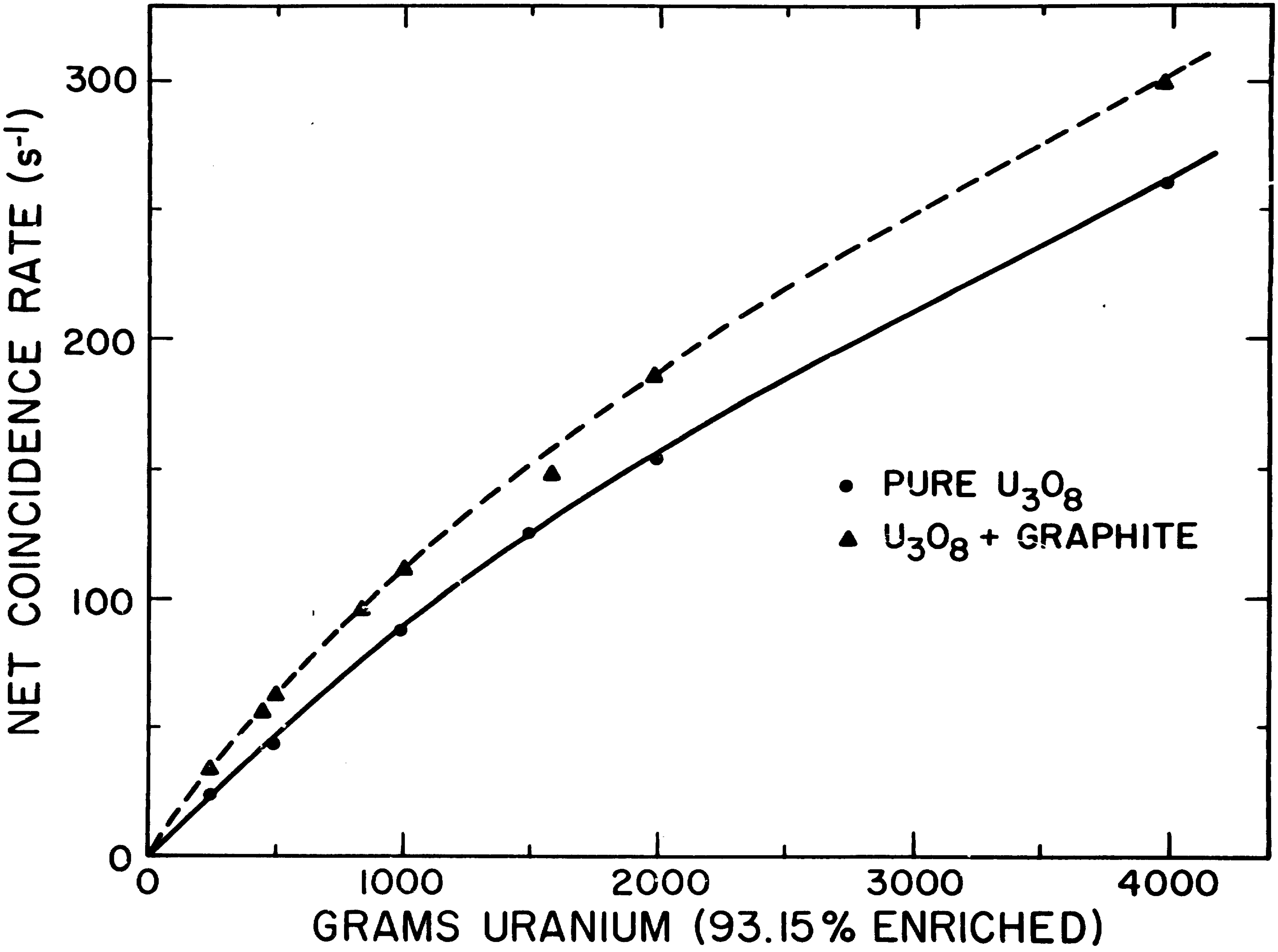

NET COINCIDENCE RATE (s^{-1})
300
200
100
0
0
1000
2000
3000
4000
GRAMS URANIUM (93.15% ENRICHED)
● PURE U_3O_8
▲ U_3O_8 + GRAPHITE

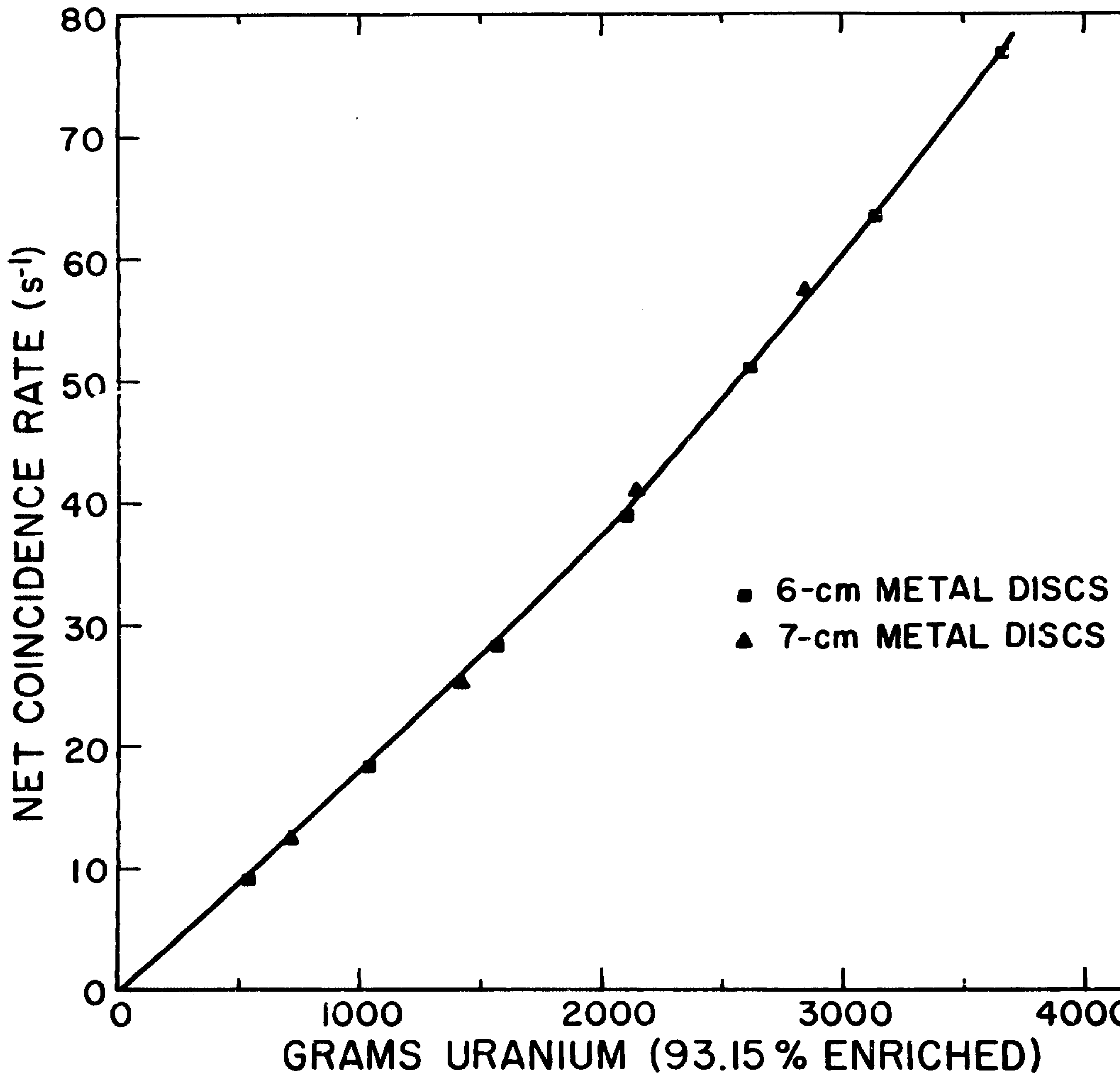

80
70
60
50
40
30
20
10
0
0
1000
2000
3000
4000
NET COINCIDENCE RATE (s-1)
GRAMS URANIUM (93.15 % ENRICHED)
6-cm METAL DISCS
7-cm METAL DISCS

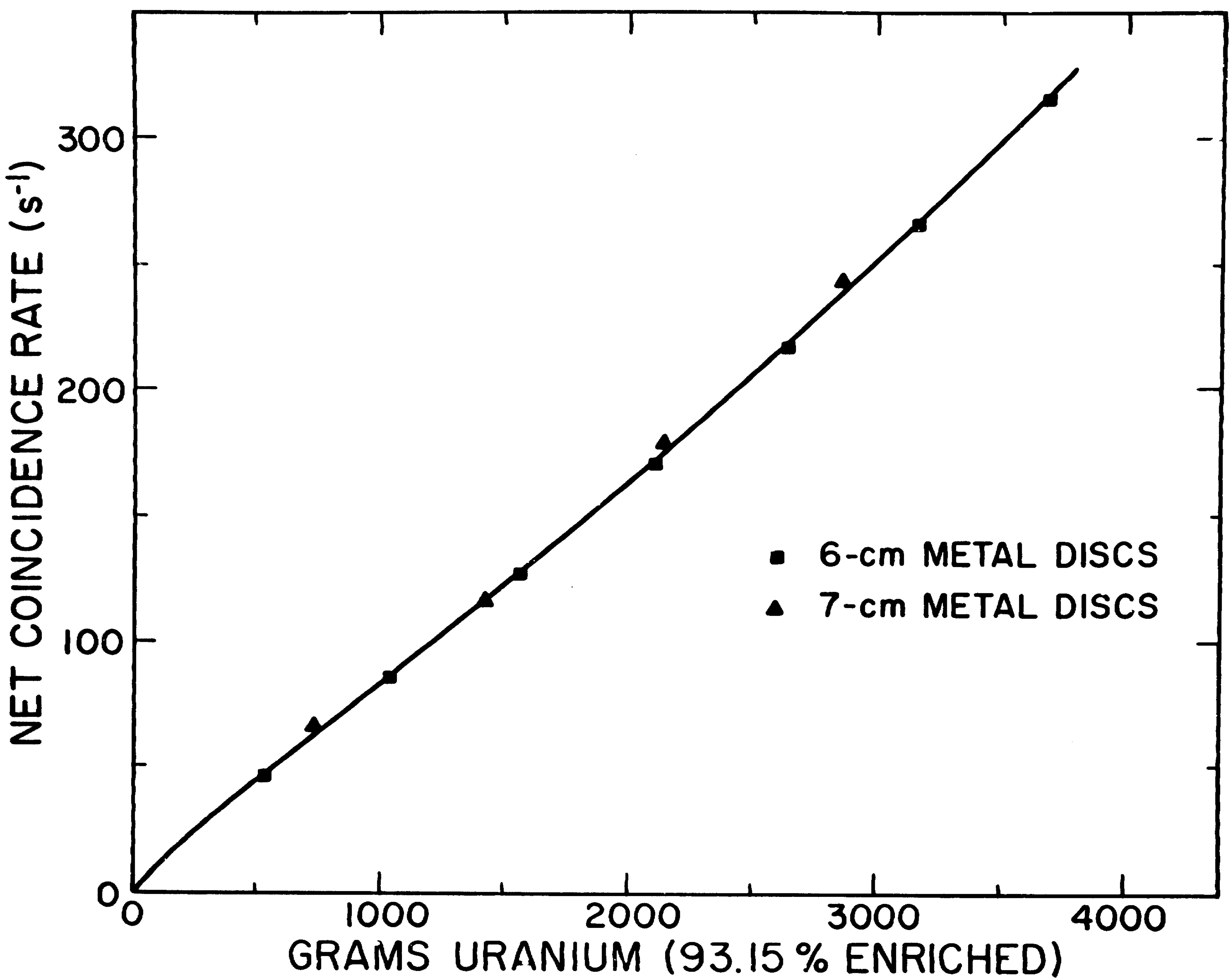

NET COINCIDENCE RATE (s^{-1})
300
200
100
0
0
1000
2000
3000
4000
GRAMS URANIUM (93.15 % ENRICHED)
6-cm METAL DISCS
7-cm METAL DISCS